Fission Cross Section of U^{235}†

C. D. BOWMAN, G. F. AUCHAMPAUGH, AND S. C. FULTZ
Lawrence Radiation Laboratory, University of California, Livermore, California
(Received 8 August 1962; revised manuscript received 28 January 1963)

The fission cross section of U^{235} has been investigated with high resolution between 0.03 and 60 eV using the neutron time-of-flight facility at the Livermore linear electron accelerator. Normalization of the relative cross sections in the thermal region indicates that the fission cross sections generally accepted are about 20% too large in the region between 5 and 60 eV. Values for $\sigma_0\Gamma_f$ and Γ_f above 5 eV are compiled and are compared with similar measurements by other investigators. Evidence is also presented which indicates that the fission widths fall into two groups probably related to the two total angular momenta involved in the reaction.

INTRODUCTION

ALTHOUGH both the fission and the total cross sections of U^{235} have been carefully studied, a much wider variation in the fission widths still exists among the different experiments than is desired from either the nuclear physics or engineering point of view. The absolute accuracy is also in question since the best measurements[1,2] of fission widths obtained above 5 ev are based on successive normalizations of different sets of data in several overlapping energy intervals extending into the thermal region. Such a procedure is satisfactory in the region below a few eV where the results between different labs are in quite good agreement. However, the quality of the measurements with the crystal spectrometer technique which extend up to[3] 10 eV decreases quite rapidly above a few eV. It is in the region from 5 to 10 eV that the relative cross sections of high-resolution measurements above 10 eV have been normalized. In view of the possibility of considerable error here, it is desirable to extend the high-resolution measurements above 5 eV into the thermal region where a direct normalization can be made to the accepted standard for the fission cross section.

The fission cross section in the region from 0.03 to 60 eV has, therefore, been measured with high resolution using the time-of-flight facility at the linear electron accelerator. A comparison of the resonance parameters with those of other laboratories is given. Evidence is also presented which indicates that the fission widths fall into two groups probably related to the two total angular momenta involved in the reaction.

EXPERIMENTAL ARRANGEMENT

In Fig. 1 the arrangement of the accelerator, the neutron target, and the flight tubes is shown. The linear electron accelerator produces pulses of 26-MeV electrons at repetition rates up to 200 pps, with widths variable from 0.025 μsec to 2.0 μsec, and with a maximum current of 0.25 A. A large fraction of beam current passes through a $1\frac{1}{4}$-in.-diam carbon collimator located 45 ft from the accelerator. It then strikes a natural

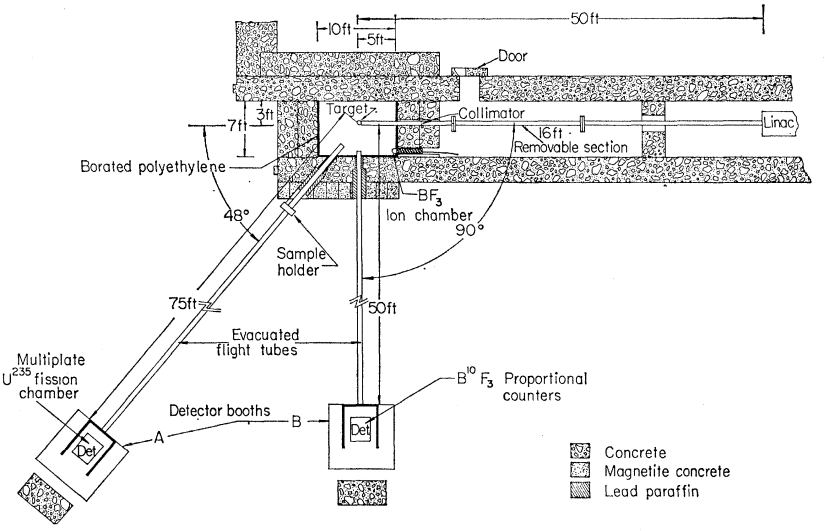

FIG. 1. Diagram of the experimental arrangement.

† This work was performed under the auspices of the U. S. Atomic Energy Commission.
[1] W. W. Havens, Jr., E. Melkonian, L. J. Rainwater, and J. L. Rosen, Phys. Rev. **116**, 1538 (1959).
[2] A. Michaudon, R. Bergere, A. Coin, and R. Joly, J. Phys. Radium **21**, 432 (1960).
[3] F. J. Shore and V. L. Sailor, Phys. Rev. **112**, 191 (1958).

uranium target 5 ft beyond the collimator, which is located roughly in the center of a concrete shielded cell.

The uranium target shown in Fig. 2 consists of an aluminum-clad uranium slug, $2\frac{1}{2}$ in. in diameter and weighing about 2.9 kg. Bremsstrahlung from the slowing down of the electrons in uranium produces neutrons by the (γ,n) and (γ,f) reactions at a rate (during the 250-mA electron pulse) of about 2×10^{16} neutrons/sec. These neutrons are moderated somewhat by a $\frac{3}{4}$-in. layer of transformer oil surrounding the target. The oil, which also serves as a coolant, is continuously circulated through a heat exchanger. This moderator has been found to be superior to both beryllium and Lucite moderators in terms of epithermal yield and neutron background.

The target is located roughly at the center of a 7 by 9 by 10-ft concrete cell which is enclosed on three sides by a minimum of 5 ft of concrete and on the fourth side, through which the flight tubes pass, by 3 ft of concrete and 2 ft of high-density magnetite concrete blocks. The roof consists of $1\frac{1}{2}$ ft of concrete covered by 1 ft of a lead-paraffin mixture of density 4. The inner walls of the neutron cell are lined with a $\frac{5}{16}$-in. layer of borated polyethylene to absorb neutrons that have been reflected from the walls back into the neutron cell.

Two evacuated flight tubes, 25 and 17 m in length, are provided at angles of 48 and 90° with the electron beam direction. A sample inserter is provided in the 48° flight tube. As illustrated in Fig. 3, considerable attention has been given to the flight-tube construction at the wall so as to obtain favorable beam definition and background conditions. The neutron beam is further collimated by several iron collimators located at various positions along the flight tube. The beam profiles in the 48 and 90° tubes, as measured by a bare BF_3 proportional counter, were found to be 10 and 8 in. in diameter, respectively, at the flight-tube terminations. The energy dependence of the neutron flux has also been measured in each tube using BF_3 proportional counters. The ratio of these measurements (at various neutron energies) for the two flight tubes was found to be constant to within 3% for energies up to 250 eV.

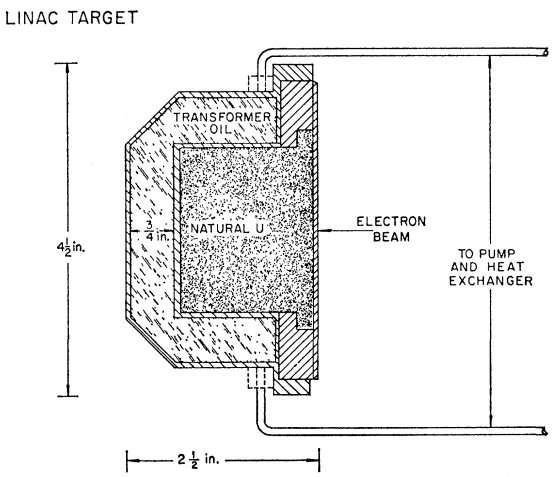

FIG. 2. The natural uranium target and moderator.

Detector booths are provided for both flight tubes. Each booth has a concrete beam stopper located immediately behind it. To insure adequate shielding from extraneous neutron backgrounds arising from leakage through the shielding of the neutron cell, each booth contains a 3 ft×3 ft×5-ft frame covered with several layers of borated polyethylene and also with boracic acid. A $\frac{1}{32}$-in. layer of cadmium can be placed in the neutron beam to prevent mixing of the slower neutrons from one pulse with the faster neutrons of the following pulse at high repetition rates.

ELECTRONIC TIMING SYSTEM

The measurement of neutron flight times was accomplished by use of time-to-height converters and multichannel analyzers. This method offers continuous variability of time-channel widths, hence broadens the choice of energy ranges in which measurements may be made with good resolution.

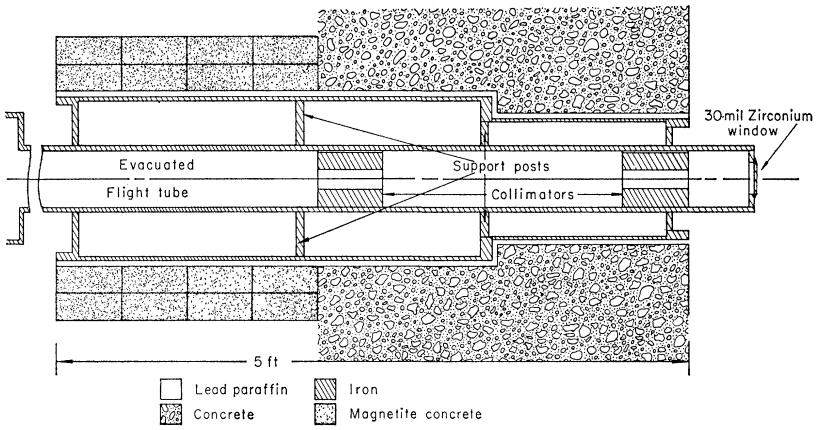

FIG. 3. Diagram of flight tube construction in the wall of the neutron cell, showing neutron shielding and collimation.

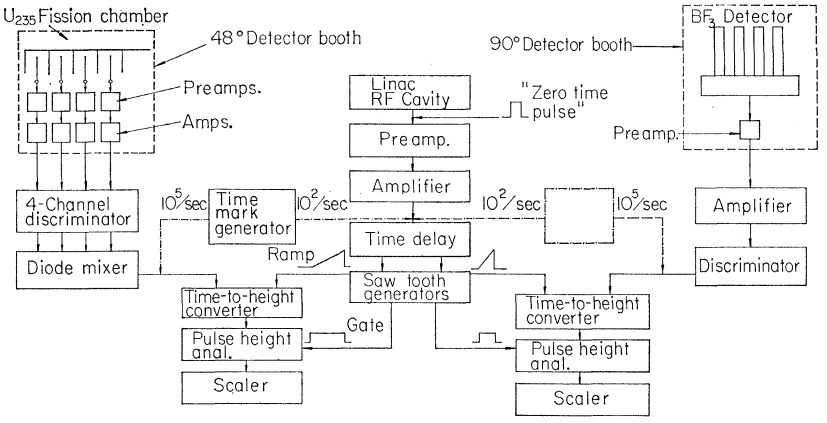

FIG. 4. Block diagram of the time-of-flight electronics.

A block diagram of the entire time-of-flight electronics is given in Fig. 4. The circuitry is duplicated where necessary so that simultaneous measurements can be made using both flight tubes. Several channels of preamplifiers and amplifiers are located in each detection booth, to be used for experiments in which they would improve the signal-to-noise ratio, or the time resolution. Pulses from the neutron detectors must travel about 200 ft from the detection booths to the control room in which the remainder of the circuitry is located. There the pulses pass through amplifiers and pulse-height discrimination circuits, after which they are mixed and fed into the time-to-height converter.

The zero-time fiducial signal is obtained by use of a tuned cavity at the output end of the accelerator. The electrons passing through the cavity are bunched by the rf (3000 Mc/sec) with approximately 3 bunches per nsec. The envelope of the rf voltages induced in the cavity can be rectified and used as a timing pulse. After amplification, the signal is delayed by means of a magnetostrictive delay line. Delays up to 600 μsec can be selected in increments of 50 μsec, while those up to 1800 μsec can be selected in 100-μsec intervals. Several different delayed pulses originating from the same zero-time pulse can be obtained, if needed. The delayed pulses are next fed to an oscilloscope trigger which provides a fine adjustment of the time delay. The oscilloscope then simultaneously generates saw-tooth and gate voltages independently variable in width from 1 μsec to 1 sec. These voltage pulses are applied to the time-to-height converter and a pulse-height analyzer, respectively.

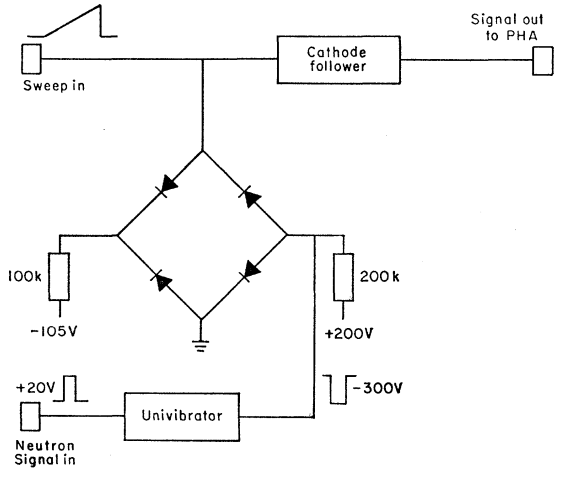

FIG. 5. Block diagram of the time-to-height converter.

A diagram of the electronics of the time-to-height converter is given in Fig. 5. The converter operates by sampling the saw-tooth or ramp-shaped voltage signal. Normally this ramp signal is, in effect, shorted to ground through a diode bridge, which is kept in a heavily conducting state through the application of 300 V dc across it. If, however, the diode bridge ceases to conduct, the ramp voltage will appear on the grid of the cathode follower and at its output. It can be made to cease conduction momentarily by the application of a 300-V pulse of opposite polarity to that of the dc supply. Such pulses are generated in the univibrator by signals from the neutron detectors. The output pulses from the cathode follower then have an amplitude proportional to the height of the ramp pulse at the instant that it was sampled. The pulses are recorded by pulse-height analyzers.

The relation between channel number and flight time is established by inserting a time-mark generator as shown in Fig. 4. The time-mark generator is calibrated by beating its oscillator against the carrier frequency of radio station WWV. In this arrangement the time-to-height converter is pulsed by a train of pulses 10 μsec apart which recur 100 times each sec. This system, of course, enables one to check linearity and stability simultaneously with time calibrations. Small corrections in the determination of the zero-time fiducial due to differing delays in the preceding circuitry can be measured by observing (γ,f) pulses induced in the fission chamber by the bremsstrahlung burst with due consideration being given to gamma-ray and electron flight times.

The stability of this system has been found to be quite satisfactory. Jitter on the short delay and magnetostrictive delays combined was about ±15 nsec in 1800 μsec, or about 1 part in 10^5. Stability of the ramp generator was considered to be better than 1 part in 10^4. The magnetostrictive delay was designed such that its temperature gradient does not exceed 5×10^{-6} (5 parts per million) per °C in the temperature range from −10 to +60°C. It was used in a temperature-stabilized room.

FISSION MEASUREMENTS

The fission cross section of U^{235} was measured between 5 and 60 eV by use of a multiple-plate ionization fission chamber which was located in the 48° detection booth at a distance of 75 ft from the uranium target. The plates were coated with a thickness of 0.5 mg/cm² of U^{235} enriched to 93% and were spaced 0.2 in. apart. A maximum of only 9 of the 25 fission plates, corresponding to a detector thickness of 1.6 in., was used due to resolution considerations. The chamber was filled to a pressure of 2 atm with a mixture of argon and CO_2 in the ratio of 19 to 1. Four BF_3 proportional tubes filled to a pressure of 15 cm of Hg were located in the 90° detection booth with their axes perpendicular to the flight-tube axis. In this way it was possible to provide simultaneous measurements of the fission and open-beam time spectrum.

To keep the neutron resolution comparable to the Doppler width, it was necessary to make several measurements under different operating conditions since the neutron yield and flight time vary fairly rapidly with energy. The required conditions are summarized in Table I. Operating conditions are not shown for the lower resolution open-beam measurements performed with the BF_3 counters in the 90° flight tube. The complete set of fission and open-beam measurements required a total of about 40 h of accelerator time for satisfactory statistics; 7600 and 5900 counts were accumulated in the peak channels of the 8.84- and 19.3-eV resonances. The statistical errors in Run C were somewhat larger than those of Runs A and B. At no time was the detection rate high enough to cause observable distortion of time spectra attributable to analyzer dead time. The ratio of fission counts vs time spectra to the open-beam counts vs time spectra gives curves proportional to $\sigma_f\sqrt{E}$ under the assumption of a $1/V$ dependence of the BF_3 counter efficiency. The curves so obtained were then joined by matching the overlap regions of the different runs starting with Run B_1.

The background in the 1- to 60-eV measurements has been determined by transmission experiments on thick rhodium and tantalum samples using both the fission chamber and BF_3 chamber as detectors. A sufficient thickness was used so that less than 0.1% of the incident neutrons would be transmitted in the wide and completely resolved resonance of Rh at 1.26 eV and the 4.4-, 10.0-, 23.5-, 36-, and 40-eV resonances of tantalum. The true cross section is obtained from the observed cross section, if the background is small, using the relation $\sigma_f E^{1/2}=(\sigma_f E^{1/2})_{obs}[1-(F_f-F_b)]$, where F_f and F_b are the background fractions measured with the fission and BF_3 detectors, respectively. Since F_f is implicitly dependent on $\sigma_f\sqrt{E}$, the sign of the correction varies and is positive on the peaks of resonances and negative in the valleys. However, the corrections at no point exceed 5% and are on the average about 3%. No corrections therefore have been made to the data. Details on the background measurements are given in the report UCRL-7061.[4]

TABLE I. Experimental conditions for high-resolution measurements.

Run[a]	Energy range (eV)	Channel width (μsec)	Pulse width (μsec)	Detector thickness (cm)	Resolution (μsec/m)
A_1	4.5–10	1	0.5	2.0	0.040
A_2	9 –20	0.5			0.035
B_1	18 –31	0.25	0.25	1.0	0.015
B_2	28 –41	0.25			0.015
C	39 –60	0.15	0.08	0.5	0.0075

[a] Two separate time-analyzing systems were used in Runs A and B for the different energy regions.

Cross-Section Normalization

The ordinate of the resulting curve was first normalized following the procedure used by Havens, Melkonian, Rainwater, and Rosen at Columbia University[1] and by Michaudon, Bergere, Coin, and Joly at Saclay.[2] The areas under the 6.42-, 7.14-, and 8.84-eV peaks were compared individually with the same peaks in the data of Shore and Sailor[3] obtained by use of a neutron diffraction spectrometer. The internal consistency among the three ratios is 10%. It will be shown later that the average values for $\sigma_0\Gamma_f$ agree with the results of Columbia and Saclay to about 5%.

Although reproducibility among the different laboratories can be obtained using this normalization procedure, the absolute accuracy is still limited by the uncertainty in the crystal spectrometer data. An additional set of measurements was, therefore, taken to extend the present measurements into the thermal energy region where a direct normalization can be made to the accepted international standard for the U^{235} thermal fission cross section.

At this point it is useful to consider the effects on the cross section of any background that might be present below 5 eV. If the number of essentially monoenergetic neutrons that appear at the detector in some time interval of width Δt are denoted by F, and the number of background neutrons in the same time interval by G, the probability (assuming no self-protection) for detection of an event in the fission chamber will be proportional to $\sigma_f F+\sigma_f' G$, where σ_f denotes the fission cross section of U^{235} and σ_f' is the

fission cross section at the energy of the background. Similarly, the probability for detection of an event in the BF_3 proportional counters is given by $\sigma_b F+\sigma_b' G$. The ratio of these two probabilities, which is proportional to the observed $\sigma_f\sqrt{E}$, can be expressed in the form:

$$\sigma_f\sqrt{E} \propto \frac{\sigma_f}{\sigma_b}\left[1+\left(\frac{\sigma_f'}{\sigma_f}-\frac{\sigma_b'}{\sigma_b}\right)\Big/\left(\frac{F}{G}+\frac{\sigma_b'}{\sigma_b}\right)\right]. \quad (1)$$

It can be shown that the validity of Eq. (1) is not impaired if an energy distribution of background is present in the interval Δt rather than a discrete energy background as in the case worked out above.

It is clear that when $\sigma_f'/\sigma_f=\sigma_b'/\sigma_b$, the background, regardless of its magnitude, does not affect $\sigma_f\sqrt{E}$. If all four variables of this relation follow a $1/V$ dependence, this relation holds. In the following discussion it will be shown that where there can be appreciable background, the background energy is such that this condition is satisfied.

Two measurements were required to extend the data into the thermal region. The first measurement in the 1.5- to 8-eV region, taken at 180 pps (pulses/sec) with the Cd filter in position, was required to bridge the gap between the near-thermal and the 5- to 60-eV measurements. The second, covering the region from 0.03 to 2.5 eV, was made with the Cd filter removed and at a pulse rate reduced to 10 pps. In these measurements the BF_3 spectra were recorded with the BF_3 detectors placed immediately in front of the fission chamber in the 48° booth. The fission measurements were carried out with the BF_3 chambers removed.

The amount of background present with the Cd filter in the beam has been measured, as mentioned earlier, by studying the transmission of a thick tantalum sample. The background in the 1.5- to 8-eV region never exceeds 3%. The problems of background for the region near thermal energy are much more severe when the Cd filter is removed. By operating the accelerator at a pulse rate reduced to 10 pps, the problem of the overlapping of neutrons can be eliminated since these backgrounds would have an energy below 0.0003 eV. However, background due to other sources must also be investigated. The first step was the observation of the effect of Cd on the open-beam neutron spectrum. The count rates from the fission chamber and BF_3 counters were measured with and without the Cd filter. The background below the Cd cutoff arising from neutrons with energies higher than the Cd cutoff was found to be less than 0.1% for both detectors. The background at neutron energies of 0.2 eV and below, which still may be appreciable, must therefore have an energy less than 0.2 eV. Since the fission cross section below 0.2 eV follows roughly a $1/V$ dependence, the relation $\sigma_f'/\sigma_f=\sigma_b'/\sigma_b$ is approximately satisfied and the effect of large backgrounds on the measurements is significantly reduced. For instance, the effect on the cross section at 0.1 eV produced by a background as large as 20%, which is distributed uniformly in energy from 0.1 down to 0.025 eV, is 2.5%.

The data in the 0.03- to 5-eV range are shown in Fig. 6. The measurements from 0.03 to 2.5 eV were normalized by matching the cross sections near thermal energy as shown in the inset. The solid curve in the inset represents the data from BNL-325.[5] The 1.5- to 8-eV measurement was joined to the lower energy data by matching the level of the curves in the overlap region from 1.5 to 2.5 eV. The background near the overlap region was measured by transmission studies of the 1.26-eV resonance in Rh using a sample 0.016 in. thick. The thickness was sufficient to realize a transmission less than 0.001 in the minimum and yet transmit at least 90% of the neutrons in the wings on either side. Backgrounds were measured under the same conditions for the 1.5- to 8-eV region using a pulse rate of 200 pps and a Cd filter in the beam. Both the fission chamber and the BF_3 chambers were used as detectors. The measurements were repeated with the Cd filter removed and at a pulse rate of 10 pps for the 0.03- to 2.5-eV measurements. The background corrections to the

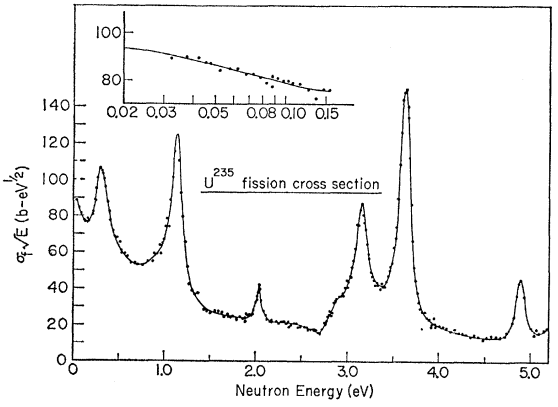

FIG. 6. The fission measurements in the 0.03- to 5-eV region. The region where the cross sections were matched between 0.03 and 0.15 is shown in the inset. The solid curve in the inset was taken from BNL-325.

TABLE II. Comparison of the normalization procedures.

E_n (eV)	$(\text{Area})_{cs}$[a] (b-eV)	$(\text{Area})_{th}$[b] (b-eV)	$(\text{Area})_{th}/(\text{Area})_{cs}$
4.90	5.5	4.7	0.85
6.45	64	53	0.83
7.20	38	30	0.79
			Av=0.82

[a] These areas are based on the normalization to the crystal spectrometer data of Shore and Sailor[3] in the 5- to 10-eV region.
[b] These areas are based on the normalization to the fission cross section in the thermal region.

[4] C. D. Bowman, G. F. Auchampaugh, and S. C. Fultz, Lawrence Radiation Laboratory Report UCRL-7061, 1963 (unpublished).
[5] Neutron Cross Sections, BNL 325, 2nd ed., Suppl. No. 1 (1960).

observed fission cross section were found to be smaller than 1.5% in the overlap region for both the 0.03 to 2.5 and the 1.5- to 8-eV measurements. Therefore, the two measurements can be matched without introduction of error due to a difference in background effects. Further details of this background measurement are given elsewhere.[4]

To obtain the proper barn scale for the 5- to 60-eV region, the area under the peaks at 4.9, 6.4, and 7.2 eV of the 4.5- to 60-eV measurements which had previously been normalized to the crystal spectrometer data as explained earlier, were next compared to the area of the same resonances in the 1.5- to 8-eV measurement, which was normalized at thermal energy (5 to 8 eV not shown in Fig. 6). These data are given in Table II. The second and third columns contain the area under the peaks for the two normalizations. The fourth column, containing the ratio of the data of these columns, illustrates the good agreement of the results from the three resonances; the average, 0.82, represents the error resulting from a normalization to the crystal spectrometer data between 5 and 10 eV.

The measurements of both fission and BF_3 spectra in the 0.03- to 8-eV region and the normalization have been repeated after removing the sixteen unused plates from the fission chamber and installing a thinner cover plate to decrease the scattering effects. The total aluminum in the beam was reduced from 0.968 to 0.343 in. Although the observed cross sections near the 0.3- and 1.0-eV resonances were somewhat modified,[4] the resulting normalization of the 5- to 60-eV data was unchanged. The scattering effects, therefore, have been shown to be unimportant to the normalization. Self-protection in the B^{10} and U^{235} has been taken into account and the effects of background, if present, have been shown to be negligible. In addition, the measurements of the neutron flux with the BF_3 counters in the near-thermal region have been compared with the results from a thick Li^6I detector.[4] After correcting the BF_3 data for their $1/V$ dependence, the detectors were found to give identical results. Apparently the only

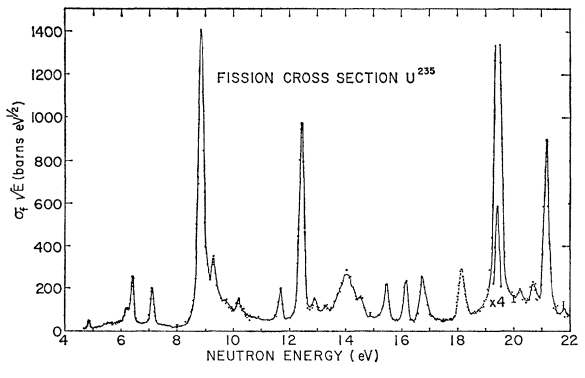

FIG. 7. The fission measurements in the 4.5- to 22-eV region. Statistical error bars computed from the number of counts per channel are also shown.

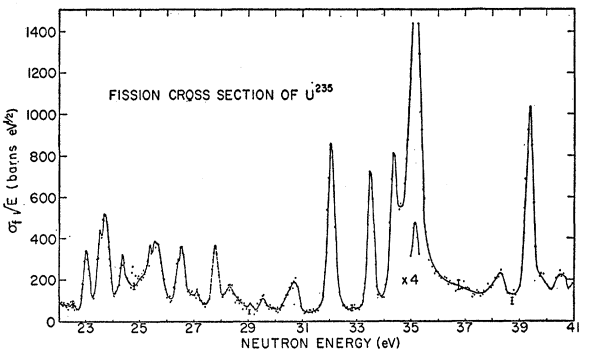

FIG. 8. The fission measurements in the 22- to 41-eV region.

significant inaccuracy in the normalization is in the joining of the different measurements. Therefore, the normalization of the cross section in the 5- to 60-eV region should be accurate to at least 5%.

The $\sigma_f\sqrt{E}$ vs neutron energy E_n curves are shown in Figs. 7, 8, and 9. The solid curve through the experimental points is broken near 18 and 28 eV since resonances in cadmium appear here, but have not been taken into account. Statistical error bars, computed from the total count per channel, are indicated throughout the figures.

ANALYSIS

The results of the analysis for resonance parameters are given in Table III. The energies at which resonances are observed are given with an accuracy of ± 0.05 eV in the first column. The energy corresponding to the peak of the resonance has been taken as the resonance energy even though interference is evidently present in several resonances. In Fig. 10 the number of resonances below a given energy E are plotted vs E. Apparently, the experiment begins to miss levels above 35 eV. The average level spacing is 0.64 eV in agreement with the determination by total cross section.[6]

Since the resonances shown in Figs. 7 and 8 are

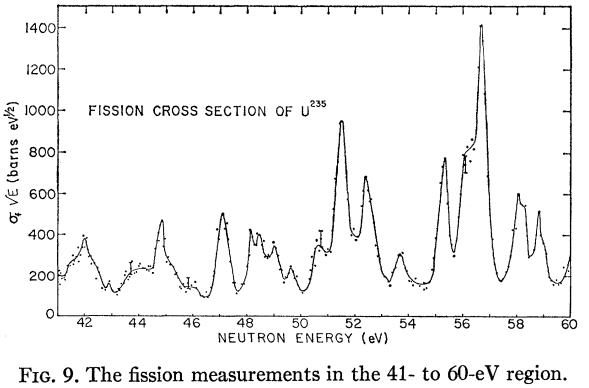

FIG. 9. The fission measurements in the 41- to 60-eV region.

[6] V. E. Pilcher, J. A. Harvey, and D. J. Hughes, Phys. Rev. **103**, 1342 (1956).

TABLE III. Resonance parameters from area analysis.

E_n (eV)	$\sigma_0\Gamma_f$ (eV-b) LRL	Columbia	Saclay	$\langle\sigma_0\Gamma_f\rangle_{av}$ (eV-b)[a]	$\langle\sigma_0\Gamma\rangle_{av}$ (eV-b)[b]	Γ_f (10^{-3} eV) LRL[c]	Mean[d]
4.85	1.5				14.7	2.9	3.3[e]
5.50							
6.20	1.8	3.8		2.7	5.7	12	20.8
6.40	12.4	9.8		12.1	57	7.2	6.7
7.10	10.8	6.6		9.1	19	31	20.1
8.85	112	89.7	105	102	148	54	39.8
9.30	7.6	20.0	17	14.7	17.1	19	70.2
9.75	1.1		3	2.0	6.7	4.1	10.4
10.10	4.6	5.2		4.9	7.3	35	37.9
10.20	2.8		5	3.9	8.2	13	20.1
11.50							
11.70	6.0	5.5	6.0	5.8	76	2.3	2.1
12.45	42.0	38.8	47	42.6	143	10.1	10.1
12.90	2.1		3.5	2.8	5.1	17	25.0
13.30	1.2		3.3	2.2	9.6	3.7	7.1
14.00	25.4						
14.55	1.5	7.4	5.0				
14.95							
15.45	8.2	6.8	9.2	8.1	20	17	15.5
16.15	7.4	5.9	10.0	7.5	27	9.5	9.2
16.70	11.6	8.7	14.4	11.6	21	27	25.2
18.10	12.9	14.2	17	14.7	24	25	30.8
19.40	102	107	106	105	195	25	24.4
20.20	2.5		5	3.8			
20.70	5.2	8.6	5	6.3	23	7.5	9.1
21.20	31.6	32.5	30	31.4	68	20	19.2
21.80							
22.50	0.6			0.6	5.2	2.8	3.5
23.00	10.8	12.5	12	11.8	37.9	10	10.7
23.55	2.5		5	3.8			
23.70	26.5	30.7	25	27.4	88.1	11	10.7
24.35	7.3	14.0	8	9.8	26.4	9.7	13.6
25.40							
25.60							
26.40	1.9			1.9			
26.55	13.3	18	17	16.1	25.2	25	33.7
27.15	4.1	4.8	4	4.3	5.25	59	61.1
27.80	13.7	15.0	17	15.2	34.6	16	17.6
28.30	8.4	4.2	7	6.5	17.1	22	14.0
29.10	1.6			1.6			
29.55	4.0	3	2.5	3.2	11.5	13	9.1
30.70	7.2	7	7	7.0	28.2	8.7	8.0
32.05	37.3	29.3	34	33.5	69.0	26	20.0
32.90							
33.50	25.5	31.2	23	26.6	80.6	12	11.6
34.35	26.3	53.8	33	37.7	133.2	6.3	9.6
35.15	106	111	106	108	219	22	21.3
38.25	8.4	13.5	12	11.3	5.5		
39.35	44	41.9	43	42.9	82.8	25	22.9

[a] The average of the results in the second, third, and fourth columns is given.
[b] The values for $\sigma_0\Gamma$ in this column are the average from the transmission measurements of Pilcher, Harvey, and Hughes (reference 6), and Simpson, Fluharty, and Simpson (reference 8).
[c] The LRL fission widths were obtained by using the fission width from the second column reduced by the factor 0.82, values for $\sigma_0\Gamma$ from the sixth column and a constant value for $\Gamma_\gamma = 33 \times 10^{-3}$ eV.
[d] The "mean" fission widths were obtained using the data of the fifth column reduced by the product 0.82×0.96, values for $\sigma_0\Gamma$ from the sixth column and a constant value for $\Gamma_\gamma = 33 \times 10^{-3}$ eV.
[e] This value was obtained by averaging the results of Shore and Sailor (reference 3), Pilcher, Harvey, and Hughes (reference 6), and the LRL values.

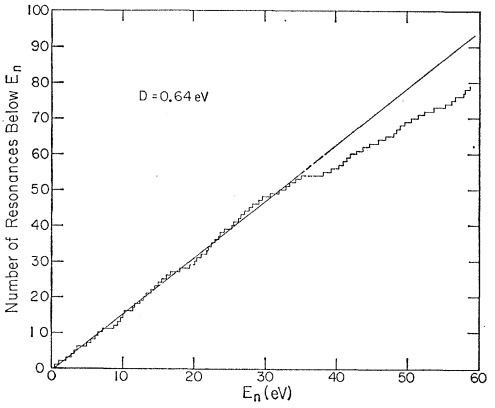

FIG. 10. The number of levels below a given neutron energy. The histogram falls away from the straight line at 35 eV, indicating a loss of levels above this energy. The straight line represents an average spacing of 0.64 eV.

fairly well separated, the width of the majority of the resonances can be determined by area analysis. However, for many of the narrower resonances the resulting parameters will have large errors. For some resonances the areas are so small and the widths so narrow that the Doppler spread almost completely obscures them, as for example around 14 eV. These effects tend to become worse as the energy increases because of the increasing magnitude of the Doppler width. For this reason the most desirable analysis, single or multilevel shape fitting, is almost impossible to apply above about 12 eV, except in the case of the larger peaks. Area analysis, which makes use of the fact that the area under a resonance is independent of the resolution and of the Doppler effect,[7] is therefore more applicable. The latter procedure does not determine Γ_f, but rather the ratio $g\Gamma_n\Gamma_f/\Gamma$, where $\Gamma=\Gamma_n+\Gamma_f+\Gamma_\gamma$. However, by using the values for $g\Gamma_n$ which are obtained from area analysis of total cross-section measurements, and by assuming Γ_γ to be constant from resonance to resonance, Γ_f can be determined. This is the procedure which has been followed here. The area A is given by

$$A=\int_{-\infty}^{\infty}\sigma_f E^{1/2}dE=\int_{-\infty}^{\infty}\{\pi\lambda^2 g\Gamma_n\Gamma_f/[(E-E_0)^2+\tfrac{1}{4}\Gamma^2]\}E^{1/2}dE=\tfrac{1}{2}\pi E_0^{1/2}\sigma_0\Gamma_f, \quad (2)$$

where $\sigma_0=4\pi\lambda_0^2 g\Gamma_n/\Gamma$. The implicit energy dependence of λ^2 and Γ_n have been included. This area was measured for all clearly defined peaks between 4.5 and 40 eV. The usual wing corrections were also applied to these areas. A tabulation of the resulting $\sigma_0\Gamma_f$ values based upon normalization to the data of Shore and Sailor is given in the second column of Table III. No errors are given on these values since it is extremely difficult to estimate the discrepancy in defining the area of closely

[7] For the thin samples used in these experiments, the influence of the Doppler effect on area is negligible.

spaced resonances with unknown interference effects. It is more useful to compare these results with those of similar experiments performed at other laboratories. This is done using the data in the third and fourth columns of Table III. The Saclay experiments were performed with the time-of-flight technique, using a linear electron accelerator as the pulsed neutron source. The Columbia measurements were taken with the same technique, but used neutrons "evaporated" from nuclei excited by high-energy protons from a cyclotron. Although the backgrounds in the experiments were different, area analysis is essentially independent of background and should, therefore, present a good basis for comparison.

As a check on the agreement of the results from the three measurements, it would seem useful to compare the deviations of $\sigma_0\Gamma_f$ for a given resonance from the average, $\langle\sigma_0\Gamma_f\rangle_{\text{av}}$, for that resonance deduced from the three sets of data. The values of $\langle\sigma_0\Gamma_f\rangle_{\text{av}}$ are given in the fifth column of Table II. For a given resonance the ratio, $\sigma_0\Gamma_f/\langle\sigma_0\Gamma_f\rangle_{\text{av}}$, has been computed for each experiment and the results plotted versus the resonance energy in Fig. 11. The individual measurements will then scatter about the dashed line at 1.0. The very small peaks with $\langle\sigma_0\Gamma_f\rangle_{\text{av}}\leq 5$ eV-b have been excluded from the plot. Agreement to within $\pm 5\%$ is apparent in the resonances at 19.4, 21.2, 30.70, 35.25, and 39.35 eV, which are major peaks and, if not well isolated from neighboring peaks, certainly represent the major influence on the cross section in their respective regions. Satisfactory agreement is also obtained for smaller but more isolated peaks where the area is also easy to define. The poorest agreements occur, as expected, for small resonances when it is necessary for the experimenter to determine the area where closely spaced resonances overlap.

As shown in Fig. 11 the average of the Columbia measurements lies on the median line. The average of the Livermore data lies 4% below, while the Saclay measurements are 4% higher. The variation in the averages could be attributed to differences in normalization or to some systematic differences in the procedure for area analysis. The standard deviation of the Livermore and Saclay measurements from the mean are about the same, i.e., ± 0.14 and ± 0.13, respectively. The deviation in the Columbia values is slightly larger at ± 0.20. The consistency of the three sets of data presented in Fig. 11 indicates that the normalization to the crystal spectrometer data by comparison of areas has been done within the 10% accuracy quoted by each of the laboratories. The sixth column of Table III contains the values for $\sigma_0\Gamma$ obtained by averaging the results of the transmission experiments of Pilcher, Harvey, and Hughes[6] and Simpson, Fluharty, and Simpson.[8] Assuming a constant value for $\Gamma_\gamma=0.033$ eV

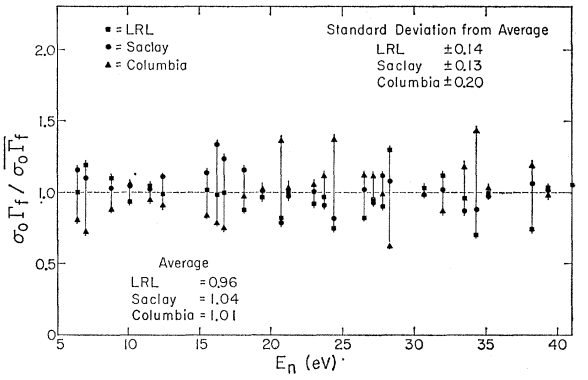

FIG. 11. The dispersion of the Columbia, Saclay, and LRL values of $\sigma_0\Gamma_f$ around the average is shown for each resonance with $\sigma_0\Gamma_f\geq 5$ b-eV. The average of $\sigma_0\Gamma_f/\langle\sigma_0\Gamma_f\rangle_{\text{av}}$ over all resonances and the standard deviation from the average is given for each laboratory.

and that $\Gamma_n\ll\Gamma_f$, the fission widths have been computed from the relation:

$$\Gamma_f=\Gamma_\gamma/[(\sigma_0\Gamma/\sigma_0\Gamma_f)-1]. \quad (3)$$

The LRL values for $\sigma_0\Gamma_f$ multiplied by the normalization constant 0.82 have been used to obtain the fission widths presented in the seventh column. Since the LRL experiment is consistent with the other two experiments, when the crystal spectrometer normalization is used, it is proper to apply the improved thermal normalization to the data of the fifth column to obtain a set of parameters of better accuracy than the LRL measurements alone. The values for Γ_f obtained from the data of the fifth column multiplied by 0.82×0.96 are given in the last column. The additional factor of 0.96 is included since the LRL values are 4% lower than the average.

The model for nuclear fission proposed by Bohr[9] and further developed by Wheeler[10] implies that slow neutron fission of an odd-A target nucleus should depend rather strongly on the total angular momentum J of the compound state. For U^{235} where the ground state spin is $\frac{7}{2}$, the two angular momenta $J=3$ and 4 occur. A smaller average width is predicted for the larger J. In spite of the fact that the distribution of fission widths for a given J are expected to vary widely, it was considered worthwhile to investigate the data for a grouping of the fission widths according to their spin. The density of the values $(\sigma_0\Gamma/\sigma_0\Gamma_f)-1=\Gamma_\gamma/\Gamma_f$ used to compute the data of the eighth column in Table III are shown in Fig. 12. It is useful to plot this value since Γ_γ/Γ_f computed in this way is not dependent on any assumptions about Γ_γ. Points representing the number of resonances in the interval $\Gamma_\gamma/\Gamma_f\pm 0.25$ are shown connected by straight lines.

[8] O. D. Simpson, R. G. Fluharty, and F. B. Simpson, Phys. Rev. **103**, 971 (1956).

[9] A. Bohr, in *Proceedings of the International Conference on the Peaceful Uses of Atomic Energy* (United Nations, New York, 1956), P/911, 2, 151.

[10] J. Wheeler, Physica **22**, 1103 (1956).

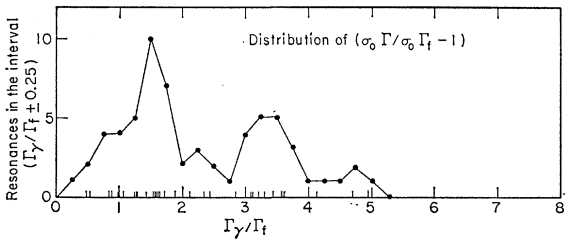

FIG. 12. The number of resonances with $(\sigma_0\Gamma/\sigma_0\Gamma_f)-1=\Gamma_\gamma/\Gamma_f$ in the interval $\Gamma_\gamma/\Gamma_f\pm0.25$ is shown vs Γ_γ/Γ_f. The value for each resonance is also shown as a vertical mark immediately above the abscissa. Only resonances between 4.5 and 40 eV are shown. The values for $\sigma_0\Gamma_f$ from the last column of Table III were used in this figure. A few resonances for which $\Gamma_\gamma/\Gamma_f>8$ are not shown.

The values for each resonance are also indicated by the vertical lines on the abscissa. Although any conclusions from these data must be especially tenuous, two peaks do seem to occur at about $\Gamma_\gamma/\Gamma_f=1.5$ and 3.5; assuming $\Gamma_\gamma=0.033$ eV for both spin states, they occur at $\Gamma_f=0.022$ and 0.0095 eV. According to the Bohr model the peak at 3.5, which includes the smaller fission widths, should correspond to $J=4$.

The fission product mass distribution is also predicted to be more symmetric for the $J=4$ group of levels than for the other group. The most extensive data on the mass asymmetry of individual resonances in U^{235} is provided by the "wheel" experiment of Cowan, Turkevich, and Browne[11] using a nuclear explosion as an intense neutron source. For 54 levels they have been able to assign a rather small but significant deviation from the average mass asymmetry. The levels fall into two groups; the more symmetric ($J=4$) occurring only half as frequently as the other group. Likewise, in Fig. 12 the areas under the two peaks occur roughly in the same ratio. Of course, more extensive data on the fission widths will be necessary to confirm these conjectures, but the indications of Fig. 12 are compatible both with the Bohr theory and the "wheel" experiment.

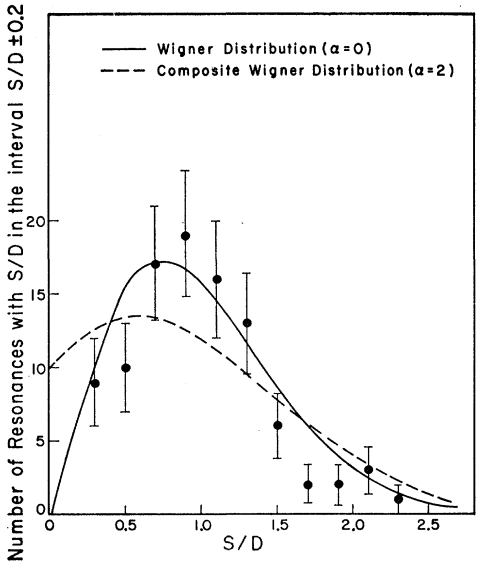

FIG. 13. The distribution of spacings below 35 eV as determined from fission cross-section measurements is shown. The curves shown are composite Wigner distributions for the two independent systems of levels. The parameter α is the ratio of the level densities.

The distribution of spacings as determined from the fission cross section of U^{235} is given in Fig. 13. These spacings are confined to the region below 35 eV. The combined spacing distribution $P(S)$ for two independent systems of levels, each of which are attributable to a spin state, is dependent on the ratio of the two level densities. However, the shape of the distribution is rather insensitive to this ratio. This can be shown by considering $P(0)$ when the probability of observing a zero spacing for either distribution alone is zero. Gurevich and Pevzner[12] find $P\alpha(0)=2\alpha/(1+\alpha)^2D$, where D is the average observed spacing and α is the ratio of the average spacing for the two spin states. It is clear that $P(0)$ is fairly insensitive to α; for instance $P_1(0)/P_2(0)=9/8$. Similarly, it can be shown that the shape of the curve $P\alpha(S)$ is rather insensitive to α. The distributions for $\alpha=2$ and 0 are shown assuming the Wigner distribution $\pi S/2D^2\exp(-\pi S^2/4D^2)$ for the individual spin states. Corrections for missed levels similar to those applied by Harvey and Hughes[13] have not been made to the data. However, if three levels have been missed in the region up to 35 eV, the points at 0.3 and 0.5 will be increased by about 20% while the other points are essentially unchanged. The spacing distribution is, therefore, not incompatible with the value $\alpha=2$ determined from the width distribution of Fig. 12.

In summary, the LRL measurements of fission widths have been shown to be consistent with the measurements of Saclay and Columbia when all three sets of data are normalized in the same way. To improve the accuracy in the normalization above 4.5 eV, the LRL measurements were extended into the thermal region where they could be matched with the accepted standard for the fission cross section. The average of the $\sigma_0\Gamma_f$ determination by the three laboratories was then corrected using the LRL thermal normalization and an improved set of fission widths computed. The distribution of fission widths indicates that there are two groups of levels at $\Gamma_\gamma/\Gamma_f=1.5$ and 3.5. This grouping is consistent with the predictions of the Bohr model for nuclear fission and with mass asymmetry measurements. Thus, the same effect which apparently

[11] G. A. Cowan, A. Turkevich, and C. I. Browne, Phys. Rev. **122**, 1286 (1961).

[12] I. I. Gurevich and M. I. Pevzner, Soviet Phys.—JETP **4**, 278 (1957).

[13] J. A. Harvey and D. J. Hughes, Phys. Rev. **109**, 471 (1958).

has been observed in U^{233} by Pattenden and Harvey[14] and perhaps in Pu^{239} by Vogt[15] is probably manifested also in U^{235}.

[14] N. J. Pattenden and J. A. Harvey, in *Proceedings of the International Conference on Nuclear Structure, Kingston, Canada*, edited by D. A. Bromley and E. Vogt (University of Toronto Press, Toronto, 1960), p. 882.
[15] E. W. Vogt, Phys. Rev. **118**, 724 (1960).

ACKNOWLEDGMENTS

The authors wish to express their appreciation to Dr. V. L. Sailor for his interest and cooperation, and to Dr. C. R. Hatcher for his assistance with the electronics. The assistance of C. P. Jupiter and P. Lane in setting up the equipment is also acknowledged.

PHYSICAL REVIEW VOLUME 130, NUMBER 4 15 MAY 1963

Alpha Decay Properties of some Holmium Isotopes near the 82-Neutron Closed Shell*

RONALD D. MACFARLANE† AND ROGER D. GRIFFIOEN‡
Lawrence Radiation Laboratory, University of California, Berkeley, California
(Received 10 December 1962)

Bombardment of Pr^{141} targets with 75- to 137-MeV O^{16} ions has resulted in the identification of new alpha-emitting isotopes of holmium. The results obtained for the alpha-decay properties of these isotopes are:

Nuclide	Alpha-particle energy (MeV)	Half-life
Ho^{151}	4.51±0.02	35.6 ±0.4 sec
Ho^{151m}	4.60±0.02	42 ±4 sec
$Ho^{152g \text{ or } m}$	4.45±0.02	52.3 ±0.5 sec
$Ho^{152g \text{ or } m}$	4.38±0.02	2.36±0.16 min
Ho^{153}	3.92±0.03	9 ±2 min

Excitation functions were obtained for the production of these nuclides and for the production of Dy^{150}, Dy^{151}, and Dy^{152}. Large differences were observed for the energy dependence of the excitation functions of the isomer pairs which were attributed to angular momentum effects. Alpha branching ratios were estimated and used to calculate alpha reduced level widths.

I. INTRODUCTION

ALPHA-DECAY systematics in the rare-earth region show that nuclides containing between 84 and 88 neutrons possess an enhanced alpha-decay energy because of the effect of the extra stability of the 82-neutron configuration. Alpha decay has been observed thus far for isotopes of the rare earth elements from neodymium to dysprosium. Most of these results have been summarized in papers by Toth and Rasmussen[1] and Macfarlane and Kohman.[2] Until the present, no extensive search has been made for the alpha decay of isotopes of the elements above dysprosium which lie near the 82-neutron closed shell although some indications have been reported. Rasmussen, Thompson, and Ghiorso observed a 4.2-min alpha activity which they believed might be due to a holmium alpha emitter[3] and Toth and Rasmussen observed an alpha activity with a half-life of a few hours which they tentatively assigned to an erbium or holmium isotope.[1]

The purpose of this paper is to report some results which were obtained on the alpha-decay properties of the 84 to 86 neutron isotopes of holmium.

II. EXPERIMENTAL PROCEDURE

A detailed description of the experimental techniques has been given in an earlier paper.[4]

A. General Procedure

Holmium isotopes were produced by $Pr^{141}(O^{16},xn)$ reactions using 75- to 137-MeV O^{16} ions from the Berkeley heavy-ion linear accelerator (Hilac). Samples for alpha-particle analysis were prepared by the electrostatic collection of recoils from a target in a helium atmosphere. Alpha-particle spectra were obtained using a Frisch-grid ionization chamber which was calibrated for energy using the alpha particles from Tb^{149}(3.95 MeV)[5] and

* This research was performed under the auspices of the U. S. Atomic Energy Commission.
† Present address: Chemistry Department, McMaster University, Hamilton, Ontario, Canada.
‡ Present address: Physics Department, Calvin College, Grand Rapids, Michigan.
[1] K. S. Toth and J. O. Rasmussen, Nucl. Phys. **16**, 474 (1960).
[2] R. D. Macfarlane and T. P. Kohman, Phys. Rev. **121**, 1758 (1961).
[3] J. O. Rasmussen, Jr., S. G. Thompson, and A. Ghiorso, Phys. Rev. **89**, 33 (1953).
[4] R. D. Macfarlane, Phys. Rev. **126**, 274 (1962).
[5] F. Asaro and J. O. Rasmussen, Lawrence Radiation Laboratory, University of California, Berkeley (unpublished results) quoted in reference 3.